Utrecht, 27 July 2020

To the Editor and Associate Editors,

Please find enclosed our response to the reviews of the manuscript 'Complementing scale experiments of rivers and estuaries with numerically modelled hydrodynamics' by authors Steven A.H. Weisscher et al. The former title was shortened for better readability.

We found the reviews constructive and helpful and will thank the reviewers in the acknowledgements.

Below we describe (in **blue**) how we will use the reviewer comments to improve the manuscript. Detailed textual comments were mostly incorporated and sometimes used as indicator where text clarity had to be improved. The revised manuscript latex text, including track changes, is attached after the reviews and authors' comments.

Kind regards, Steven Weisscher (on behalf of all authors)

REVIEWING: 1 – Laurent Lacaze

General comments:
This paper deals with the evolution of river models, including meandering river and braided river, as well as their connection to the dynamics of estuaries. The study is based on laboratory experiments performed by some of the authors and available in the literature. They are composed of two sets of experiments in two different apparatus: one focusing on the influence of fine particles on the generation of either braided river or meandering river, and the other one modelling the dynamics of the estuary. The aim of the present paper is to provide a numerical modelling of the fluid flow for these different experimental observations, in place of experimental measurements, which are hardly accessible for such complex systems. In particular, a shallow model solver, Nays2D, is used for that purpose.

From a general point of view, the paper is well written, clear, and well documented to understand the necessary background from the previous experimental paper. Moreover, the general idea of providing coupled numerical and experimental devices to describe the entire dynamics of the strongly coupled fluid dynamics and morphodynamics system makes sense and would probably be a very interesting approach to be implemented in river modelling. The obtained results are clearly presented and are shown to be of relevance with experimental observations. In particular, to prove the relevance of the modelled fluid dynamics, maps of water level difference (between numerical results and experimental measurements) are provided. Pictures and movies show that the global qualitative trend of the fluid evolution is recovered with the numerical model. The error between numerical model and available experimental data are shown to be within 10%.

Even if I feel that the general purpose of the paper would be of interest for the scientific community, I have some doubt about the scientific content required for publication in an international journal in the state. In particular, the novelty of the paper is to be found in the strategy of coupling experimental measurements with numerical models to provide a full characterisation of the system. Altogether, we imagine that the aim is to provide a global analysis of the river system then leading to a more general understanding of its genesis and its morphodynamics.

According to that, I have two major issues:
1.1) No new input is given in this paper on the understanding or description of meandering or braided rivers, according to the objective of linking a numerical model to experiments. Only a validation of the numerical model is proposed here showing somehow its relevance for this more general objective. In my opinion, it weakens the paper, and a deeper investigation of the physics of the full system using this combined approach should be proposed.
The main objective of our manuscript is to show how a numerical model, in our case Nays2D, could enrich experimental data in experiments with 1s-10s mm flow depth, i.e. close to the viscous sublayer. This approach results in spatio-temporally continuous data of water depth, flow velocity and bed shear stress, of which the latter two are difficult to be obtained from experiments by in-situ measurements. Additionally, the use of a numerical model aids in future experiment setup design as the model allows for testing different boundary conditions, thus reducing the number of tests in the lab.

This method does not change the main findings in the published experiment case studies (i.e., Van Dijk et al, 2013; Leuven et al, 2018), but makes new findings possible in the near future. Here we have shown the model to be applicable in very different experimental systems that allows answering very different scientific questions, such as the initiation of chute cutoffs (does that start on the upstream or downstream end of the pointbar?) or the reduction of tidal prism by sedimentation (does that start on the upstream end of the tidal system or everywhere at the same time?). Similar questions can now be raised in many experiments recently published. A study of the physics of those full systems is therefore well beyond the scope of this paper.

We will clarify our aim in the introduction with the proposed text under comment 2.1 of Reviewer 2.

Additionally, we will more clearly present to the reader in the discussion section how the experimental data-model integration could be used to derive new data that are difficult to acquire via in-situ measurements, as were already touched upon in the first version of our manuscript. We show that (1) maps of nondimensional bed shear stress can be linked to measured morphological change (Fig. 12 in first manuscript), and; (2) that maps of water depth and flow velocity can be used to extract tidal prism (Fig. 10 in first manuscript) and create inundation maps (Figs. 12g in first manuscript and Supplement Figure 2).

1.2) The coupling approach has already been proposed for other applications, or experimental devices. This is somehow a branch of data assimilation. Here, the method used for the numerical approach is one-way (and slightly weak), in the sense that there is no loop of control between the two approaches. The only "link" between the experimental measurements and the numerical model is to provide the final bathymetry of the river system obtained from the experiment as the initial condition for the numerical model. Then the shallow water model is run on this steady topography. I guess that more advanced coupling approach would be more appropriate. The proposed approach does not seem to be in the state of the knowledge on numerical algorithm dealing with coupling experiments and numerical modelling.

Indeed, this is a 'one-way' approach. The reviewer suggested a more advanced coupling approach would be more appropriate. Below we explain why we think this is as of yet infeasible to attain our goal of complementing experimental bathymetry data with modelled hydrodynamic data.

Firstly, we interpreted 'a more advanced coupling approach' as including the modelling of sediment transport and hence morphological change, and comparing the newly modelled bathymetry with the morphological change of the scale experiment. There are a few reasons why we have chosen not to do this.

1) Including sediment transport and morphological change goes beyond the goal of complementing experimental data and comes closer to (indirectly) substituting experiments.
2) Morphological change heavily depends on which sediment transport predictor (e.g. Meyer-Peter & Müller, 1948; Engelund and Hansen, 1967) is used and may require unrealistic parameterisations to get the morphology 'right' (Baar et al. 2019). Nonetheless, to get an indication of the amount of sediment transport and morphological activity, Nays2D produces maps of sediment mobility (i.e. nondimensional bed shear stress) that can be used for this purpose.

Baar, A. W., Albernaz, M. B., van Dijk, W. M., & Kleinhans, M. G. (2019). Critical dependence of morphodynamic models of fluvial and tidal systems on empirical downslope sediment transport. Nature communications, 10(1), 1-12.
Engelund, F., & Hansen, E. (1967). A monograph on sediment transport in alluvial streams. Technical University of Denmark 0stervoldgade 10, Copenhagen K.

Alternatively, we interpreted 'a more advanced coupling approach' as data model assimilation, which is used to improve model forecasting (e.g. bathymetric surveys, wave buoy data). However, we intend to complement bathymetric data and not forecast flow conditions at later stages in the experiment.

Regarding the comment on the use a static/final DEM, please see under comment 2.2 of Reviewer 2 for our justification and proposed text changes.

We believe the strength of the experimental data-model integration lays in applying the numerical model not just to the final DEM, but to the series of DEMs throughout an experiment. This enables the user to track the development of e.g. tidal prism, area of flood inundation and flow patterns, which are easier to acquire via the model than from measurements. In this manuscript, we present the use, accuracy and new data of the data-model integration. At a later stage, we intend to apply the integration to a series of DEMs. We will clarify this in the introduction (See under comment 2.1 of Reviewer 2).

Specific comments:

1.3) The paper is, in my opinion, too wordy regarding the available results. Most of the discussions sound a bit as assumptions on possible scenario than actual results supported quantitatively.

We use part of the discussion section to present how the reader may use the experimental data-model integration (1) to outperform measurements, and; (2) to derive new data that are normally impractical to measure in landscape scale experiments. For example, we show quantitatively how tidal prism based on measurements goes very wrong, as the law of mass conservation does not apply on the erroneous data, as opposed to modelled tidal prism. Next, a few examples are given on how the modelled data may be used to derive new information that is interesting for our reader, such as maps of inundation and maps of nondimensional bed shear stress (Fig 12 and Supplement Fig. 2).

Please see under comment 2.2 how we intend to change the discussion section.

1.4) The authors should provide relative error maps instead of absolute. In the state, I am wondering if 10% error is not an underestimation of the actual error.

The 10 % error for water depths and 15 % error for flow velocities as mentioned in the manuscript are based on the mean absolute errors given in Figures 5 and 7a. Indeed, there are locally larger errors between measured and modelled water depths. However, most larger errors correspond to incorrect measured data due to lighting overexposure, differently coloured substrate and obstacles between the experiment and measuring equipment. The point of the modelling was to avoid low quality results from measurements despite extensive filtering and extrapolation, so here we simply disregard erroneous measured data in the computation of the mean absolute errors. This is explained in the caption of Figure 5 and 9, and we will clarify this in the methods section as well (see proposed text changes below). We prefer to show the absolute values in the manuscript and added a figure to the supplement containing the relative errors.

1.5) According to the fact that topography is imposed from the experiments (from my understanding, clarify otherwise),

This is correct.

and only the fluid flow is modelled using shallow water equations, 10% error on water height (and maybe more in some places), sounds quite significant to me. As somehow mentioned by the authors, one of the weaknesses of shallow type approach is the modelling of the friction factor. This is where data assimilation would make sense for such a complex system. Could the authors justify that their one-way coupling approach makes sense, and is sufficient, in their system to provide relevance.

See under comment 1.2 and 1.4: the main error is in the measurements. For reasons of parsimony, we used a constant friction factor for the entire DEM, which ignores spatially variable friction. It is of course possible to calibrate this spatially, but then all measurement errors (lighting, sediment colour, PIV) are also attributed to friction which would be a poor application of data assimilation.

-> We will clarify our choice for a constant friction factor in the methods section.

In the discussion section we already indicate that the error could perhaps be reduced by using a spatially variable friction factor in Nays2D. This would require grain size maps of the experiment, which can be calculated from overhead imagery.

1.6) I do not understand the comment on the use of Nays2D instead of Delft3D. I am not familiar with these specific codes, but from my knowledge of shallow model, the main adjustment is on the friction model, which can indeed have an impact on the typical scales that can be solved with relevance. However, such issue regarding the maximum height that can be solved with one of the code does not make any sense to me. This is maybe a technical issue, but it cannot be a fundamental issue with this kind of approach. Could the author develop, or remove that comment, as in my opinion, they can use the shallow code they want without justification.

Yes, it is a technical issue and we will clarify this in the manuscript. We did not intend to justify the approach, but instead, we would like to explain to the reader that not all numerical models are suitable to modelling flow in scale experiments (i.e. in the order of a few mm to cm), for example due to build-in thresholds for minimum water depths. To this end, we start the methods section with our motivation for using the relatively unknown Japanese model Nays2D instead of often used models such as Delft3D and FLOW-3D.

1.7) p20. l6. I understood that no sediment transport is used in the modelling used in this paper. So, what does this remark mean here? Actually, if this is available, I would be curious to see how the system evolves from the one obtained using the experimental topography, as the fluid flow characteristics obtained numerically are probably not the ones of an equilibrium state according to the stability of the sediment bed and its evolution due to sediment transport.

The remark that Nays2D computes sediment mobility (i.e. nondimensional bed shear stress/Shields stress) is because of the following: (1) sediment mobility is an important parameter for comparison to natural systems, and; (2) it gives vital insight in sediment transport fields and morphological activity without computing actual sediment transport.

We agree with the reviewer that modelling sediment transport is an interesting step to take with our model, but we have chosen not to do this, as explained under comment 1.2. In the future, we intend to explore the sediment transport in the model versus experimental observations, but the advanced imaging techniques required for this make this well beyond the present scope.

Other comments:

1.8) p2. What does the author mean here by biomorphodynamics. Is there something I have missed here?

Biomorphodynamics involve the morphological development of e.g. a river, estuary or coast in conjunction with plants and/or animals. These living species affect the morphological development by e.g. increasing the hydraulic roughness (plants, oysters) and consolidating/stirring sediment (bioturbating animals). In turn, the flow conditions determine where these species may thrive, creating a feedback loop. In the context of scale experiments, the simulation of biomorphodynamics predominantly entails the addition of vegetation (e.g. Tal and Paola, 2007; 2010; Braudrick et al, 2009, Lokhorst et al. 2019). See for example Viles (2012) and Viles (2019) for further information on bio(geo)morphodynamics.

Viles, H. A. (2012). Microbial geomorphology: a neglected link between life and landscape. Geomorphology, 157, 6-16.
Viles, H. (2019). Biogeomorphology: Past, present and future. Geomorphology.

Upon review, we found that we only used this terminology once in the manuscript. Therefore, we will substitute 'biomorphodynamics' with 'morphodynamics' and clarify how and why vegetation may be used in landscape scale experiments.

1.9) p4. The description of the forcing flow into the Metronome flume should be improved. I had trouble to understand the tidal forcing model in the state.

We will improve the description of the tidal forcing in the manuscript and refer to the supplementary movie for visual aid. The new text will be*: … The tilting motion alternately generates a slope in the landward direction during flood and a slope in the seaward direction during ebb, which result in tidal currents strong enough to move sediment along the entire estuary (Kleinhans et al., 2017) (Supplementary movie). …*

Additionally, we will add information to Figure 2b to further clarify the setup and functioning of the flume the Metronome (additions in white: *short central axis over which the Metronome tilts*, and *up-down arrows next to the actuators to show the vertical movement of the Metronome*). Together with the text, the supplementary movie and the citation of the flume papers (i.e. Kleinhans et al., 2017; Leuven et al., 2018), we believe this to be sufficient to explain the tilting mechanism of the

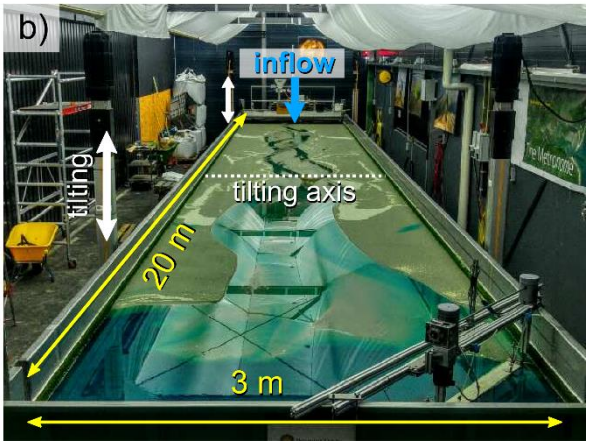

Metronome.

1.10) p7. Typo: visocosity nu instead of v, according to equation (3)
Changed.

1.11) p8. And figure 3. What is meant here by boundary conditions? “boundary” instead of input?
We distinguish between boundary and initial conditions as inputs to our model. For example, river discharge and tides are boundary conditions, which are applied throughout the model runtime, and the water depths at the beginning of the model run is an initial condition. The parameters in the box ‘Boundary conditions for numerical modelling’ are all boundary conditions.

Upon review, we will change the parameter ‘initial height’ of the downstream weir in Figure 3 into ‘mean water depth’ to avoid confusion between initial and boundary conditions.

1.12) p10. l15. computes -> computed
Changed.

1.13) p10. l22. “the model produces a single sinuous channel. . .” Two options, (i) I have missed something in the approach proposed in the paper (linked to my major comments) which therefore would require a serious revision of the paper to provide more clearly what is actually performed or (ii) the remark here is irrelevant. In case (ii), as the topography is imposed from the experiments how could it be otherwise?
Thank you for asking this question. We meant to indicate that the model shows that flow velocity and flow volume concentrate into one sinuous branch, despite (1) the multi-channel character of the DEM with cross-cutting channels over the point bars and (2) despite the considerable overbank flow. This is important but not surprising as this tendency was found in many types of systems in the literature.

We will clarify this in the manuscript. The proposed change text (changes underlined): *…Similar to the meandering river experiment, the model produces flow that is focused in a single sinuous channel,*

especially for x > 4 m (Fig. S1), despite the multi-channel character of the DEM and the considerable overbank flow. This distinction of a main sinuous channel and swale channels …

1.14) Figure 4. In my opinion, a relative error would show more than 10% discrepancy between experiments and numeric. Deeper discussions and arguments on the relevance of the numerical model should therefore be proposed.

Please see our answer to comment 1.4.

REVIEWING: 2 – Michal Tal

This paper puts forward the use of a hydrodynamic model as a robust tool for reproducing flow depths and velocities from physical experiments conducted in the laboratory in complement to the range of other measurement methods typically used (laser scans, photogrammetry, dye, point gauge, PIV). The authors compare and analyze results of a hydrodynamic model (Nays2D) with measurements conducted in two physical experiments (evolution of meandering and tidal influence on estuaries).

As a researcher with experience conducting physical experiments and more recently using hydrodynamic and morphodynamic models in field-based studies, I am familiar with the challenges, advantages, and limitations of these different approaches, and I proceeded to read this article with a keen interest in learning about the advantages offered by combining these approaches.
Thank you!

I have several general suggestions for how I think this paper can be improved to be more in line with the main goal of this paper which is to demonstrate the advantages of using numerical models as a complementary tool in experimental/physical studies.

2.1) To begin, I think the novelty of this work is a bit overstated and should be better framed within the context of other existing studies. Furthermore, the claim that there is a lack of studies combining experiments and models needs to be nuanced in order to provide more context about the novelty of this study. Classic hydraulic engineering studies based on physical models of fixed beds in combination with hydraulic numerical models have been used for decades and are not discussed. Meanwhile numerical morphodynamic models have been increasingly used in combination with physical models. Below is a very small sample of existing studies combining numerical models and physical experiments. I think that these or similar studies should be presented in the introduction and how this study clearly differs from / complements / builds on these studies discussed.
http://citeseerx.ist.psu.edu/viewdoc/download?doi=10.1.1.464.6454&rep=rep1&type=pdf
https://ascelibrary.org/doi/abs/10.1061/(ASCE)0733-9429(2004)130:3(237)
https://www.sciencedirect.com/science/article/abs/pii/S0309170812002928
https://pure.tudelft.nl/portal/files/7166802/Paper_numerical_Hirano_v2_revised.pdf
https://web.a.ebscohost.com/abstract?direct=true&profile=ehost&scope=site&authtype=crawler&jrnl=10297006&AN=140489722&h=hshWMYqLU8DImRQQKZj7%2b8e3DbzWJiQEW6lX81%2fjXbhnchpJtaMACSRzcgrI5i6SD9AwlVzPBUOwi3njgcXC8g%3d%3d&crl=c&resultNs=AdminWebAuth&resultLocal=ErrCrlNotAuth&crlhashurl=login.aspx%3fdirect%3dtrue%26profile%3dehost%26scope%3dsite%26authtype%3dcrawler%26jrnl%3d10297006%26AN%3d140489722
We agree with the reviewer that the manuscript would benefit from a clearer description of the kinds of studies that combine experiments and numerical models. We will rewrite part of the introduction to make clear how our study differs / complements / builds on other studies. Please find below a brief explanation how our approach differs from the studies presented by the reviewer. This is followed by the proposed text changes in the introduction section.

Firstly, our approach differs from experiments with flow depth of >10 cm, where topographic constraints make calculations of shallow water equations simpler, and the larger water depth allows the use of advanced measurement equipment.

Secondly, our general approach differs. In the engineering approach, comparison of the modelled and measured morphodynamics tells us mainly about the reproducibility of the experiment morphology by the model, rather than the model complementing the measured DEM with water depth and flow velocity data.

Proposed text (changes underlined): *… The focus of this study is on landscape scale experiments that simulate morphodynamics with shallow water depths of at maximum a few centimetres, i.e. in or just above the viscous sublayer. This kind of scale experiments differs from classical hydraulic flume studies*

(e.g. Struiksma et al., 1985; Neary et al., 1999) and larger scaled experiments (e.g. Zanichelli et al., 2004; Siviglia et al., 2013) with water depths >10 cm in which flow data can be more easily measured with lasers and submerged flow meters (e.g. ADCP). In contrast, data collection in landscape experiments is often difficult, infrequent and hindered by various problems (Fig. 1).

Typical data collection in landscape scale experiments targets the following three elements: (1) the morphological development from overhead imagery and digital elevation models (DEMs) from laser scanning or stereo photography on a dry bed (e.g. Ashworth et al., 2004; Hoyal & Sheets, 2009; Leduc et al., 2019); (2) water depth estimated from dye and light attenuation, possibly combined with absolute water level point measurements (e.g. Peakall et al., 2007; Tal & Paola, 2007; 2010), and; (3) flow velocity from particle imaging velocimetry on the water surface from floating particles or dye injections (e.g. Tambroni et al., 2005, Braudrick et al., 2009). Due to the shallow water depths in landscape experiments, it is technically difficult to conduct flow measurements by submerged instruments without disturbance of the sediment transport and with the same spatial resolution as of the bathymetry. To overcome the drawbacks of data collection and post-processing, there has so far been one research team (Tesser et al., 2007, Stefanon et al., 2010; 2012) that modelled water depth and flow velocity over DEMs of tidal basin scale experiments. However, the modelled data acquired by this novel method was not extensively validated against measured data and the model only applies for uniform flow conditions (Marani, 2003).

Here we explore the possibility of extending the numerical flow model application by Tesser et al. (2007) and Stefanon et al. (2010; 2012) for unsteady, nonuniform flows in landscape scale experiments. We aim to complement the measured morphological data with continuous, spatiotemporally dense numerical data of water depth, flow velocity and bed shear stress. On the one hand, this is a similar practice to modelling flow over the measured morphology of real rivers and estuaries (e.g. Berends et al., 2019), whilst here the shallow water equations need to be solved. On the other hand, this practice differs from remodelling the morphological development of a scale experiment (e.g. Struiksma et al., 1985), which are subject to all the combined errors of sediment transport predictors (Baar et al., 2019). The extended integration of experimental data and a numerical flow would not only expand the possibilities for data analyses of a series of experiment bed scans, but would also open up fast methods of testing alternative experimental settings for either an experimental or idealised morphology.

Struiksma, N., Olesen, K. W., Flokstra, C., & De Vriend, H. J. (1985). Bed deformation in curved alluvial channels. Journal of Hydraulic Research, 23(1), 57-79.
Neary, V. S., Sotiropoulos, F., & Odgaard, A. J. (1999). Three-dimensional numerical model of lateral-intake inflows. Journal of Hydraulic Engineering, 125(2), 126-140.
Zanichelli, G., Caroni, E., & Fiorotto, V. (2004). River bifurcation analysis by physical and numerical modeling. Journal of Hydraulic Engineering, 130(3), 237-242.
Siviglia, A., Stecca, G., Vanzo, D., Zolezzi, G., Toro, E. F., & Tubino, M. (2013). Numerical modelling of two-dimensional morphodynamics with applications to river bars and bifurcations. Advances in Water Resources, 52, 243-260.
Baar, A. W., Albernaz, M. B., van Dijk, W. M., & Kleinhans, M. G. (2019). Critical dependence of morphodynamic models of fluvial and tidal systems on empirical downslope sediment transport. Nature communications, 10(1), 1-12.

2.2) The work presented in this paper combines numerical models with physical models consisting of mobile beds that can evolve morphodynamically. I think this point should be presented and discussed much more explicitly, as it raises the question of the relevance and what insights are gained by using a hydraulic model with a fixed bed to compare with experiments in which the bed is continuously evolving. How often do scans of the experiment need to be conducted and the model updated in order to be able to compare the evolution? Why not compare the experiments to morphodynamic models?
We thank the reviewer for bringing this up. Morphological changes are slow relative to hydrodynamic changes so the flow model on the static DEM represents conditions over many tidal cycles. This is also

seen in numerical morphodynamic modelling where the flow time step is usually at least an order of magnitude smaller than the morphological change time step. The idea of our model is to apply it in the future to a series of bed scans, but not to try and predict the morphological change, which would be subject to all the combined errors of sediment transport predictors. Using a fixed bed is therefore no issue here.

-> We will clarify this in the introduction (see proposed text under comment 2.1) and in the discussion section of our manuscript.

2.3) Beyond the direct comparison of the numerical and experimental data, which are interesting, I do not think the paper goes far enough in analyzing and "selling" the added benefits of using a hydrodynamic model and evaluating the cost-benefits in terms of the time investment and insights gained. In other words, I came away from the paper without a clear conviction that combining these approaches is worth the investment and that the gains from taking a combined approach surpass the results of using only one approach (numerical modelling or physical experiments). I think the authors can go further in their analyses and discussion to make a stronger case for what this paper argues for: that experimental data-model integration allows for experiments to be conducted in a manner requiring fewer measurements and less post-processing in a simple, affordable and labour-inexpensive manner. I think that part of the problem stems from the fact that the paper relies heavily on the details of physical experiments conducted and published previously. While I have no problem with the author's applying a numerical model to previously vetted and published experiments, the details of the experiments and the measurements presented here are insufficient to evaluate the steps and investment in acquiring them. The insights gained by applying a numerical study to experimental data that already exists from a previous study is not necessarily equivalent to the cost/benefits of designing new (future) experiments that integrate both methods at once. While the authors make a good argument for how these approaches and data sets complement / complete each other, they do not go far enough in demonstrating that the combined approach yields results that are greater than the sum of its parts (i.e., results of two separate studies/approaches). Given that all studies are limited in time and resources this point seems very relevant when designing a study. I encourage the authors to be more creative in analyzing and presenting their results in order to make this argument more compelling by, for example, specifying the new insights that were gained into how the system behaves/evolves by using a combined approach versus just one or another, and/or how using the numerical model cut down the need for measurements.

We thank the reviewer for the feedback and we will clarify and emphasise in the discussion section (1) how the numerical model complements the experiment, and; (2) how the model may be used for experimental setup design. Please see below our comments on (1) and (2).

(1) Since the numerical model requires a static bathymetry of an experiment DEM, the numerical study is integrated with the experiment study and therefore cannot be seen as a completely separate study but more as a complementation to the experiment. The model allows for the calculation of hydrodynamics of full spatial coverage that adhere to mass continuity, unlike in-situ measurements of water depth and flow velocity. So, parameters such as tidal prism and tidal excursion length may be computed much more accurately with modelled data (see Fig. 10 in first version manuscript that shows how wrong this goes if based on in-situ measurements). Additionally, the model produces maps of bed shear stress that give insight in sediment transport fields.

Instead of estimations, these parameters and others that may be derived from the modelled hydrodynamics can now be quickly calculated. And if the model is applied to a series of DEMs, one may come to a more quantitative and more complete interpretation the development of the hydrodynamics.

-> We will emphasise how new parameters, such as tidal prism, can be calculated from the modelled data.

-> We will clarify to the reader that the experimental data-model integration may be used to a series of DEMs to track the development of its hydrodynamics over time (see also our comment to comment 2.1 by Reviewer 2).

(2) The design of a flume experiment normally requires a number of tests that need to be done in series before the 'actual' experiment is run. Parameters such as input discharge, downstream water level and downstream flume slope may need testing to get the desired setup.

The benefit of testing these parameters in the numerical model is twofold. Firstly, the initial and boundary conditions can be tested *in parallel*. Based on the resulting flow fields and bed shear stress maps at the start of the modelled setups (sediment transport is not included), preferred flume settings may be readily derived and applied to the physical flume. Therefore, most probably fewer tests are required in the physical flume, which greatly reduces the total lab time. This is especially the case for experiments with different sediment mixtures and with vegetation, for which the flume needs to be emptied and cleaned after every run. This requires the parameterisation of vegetation in the input roughness maps.

Secondly, water depth and flow velocity measurements that are commonly done near the time stamps the DEMs, are no longer required, apart from a few measurements for model validation. This is, because the hydrodynamic data are generated by the model. Therefore, less time is needed for acquiring and post-processing measured data, which cuts down time spent in the lab and/or speeds up the lab work.

-> We will clarify in the manuscript how flume design settings can be tested by the numerical model and how this reduces the iteration to the desired experiment setup and settings.

2.4) Finally, I recommend that the order of sections 2.2. and 2.1 either be reversed or that section 2.1. be moved to the methods so that the flow of the paper moves from the introduction and overview of techniques to the methods and specific setup of the experiments used in this study.

We will change the order of sections 2.1 and 2.2 and will make small text changes to maintain the flow of text.

TRACK CHANGES IN MANUSCRIPT

%% Copernicus Publications Manuscript Preparation Template for LaTeX Submissions
%% ---------------------------------
%% This template should be used for copernicus.cls
%% The class file and some style files are bundled in the Copernicus Latex Package, which can be downloaded from the different journal webpages.
%% For further assistance please contact Copernicus Publications at: production@copernicus.org
%% https://publications.copernicus.org/for_authors/manuscript_preparation.html

%% 2-column papers and discussion papers
\documentclass[esurf, manuscript]{copernicus}

%% \usepackage commands included in the copernicus.cls:
%\usepackage[german, english]{babel}
% \usepackage{tabularx}
%\usepackage{cancel}
\usepackage{multirow}
%\usepackage{supertabular}
%\usepackage{algorithmic}
%\usepackage{algorithm}
%\usepackage{amsthm}
%\usepackage{float}
%\usepackage{subfig}
%\usepackage{rotating}
\graphicspath{ {Figures/} }

\begin{document}

%%
%%%%%%%%%% TITLE PAGE %%
%%
\title{~~Implementing a hydrodynamic model to complement water depth and flow velocity data for physical~~Complementing scale experiments of rivers and estuaries with numerically modelled hydrodynamics}

\author[1]{Steven A.H. Weisscher}
\author[1]{Marcio Boechat-Albernaz}
\author[~~1~~2,3]{Jasper R.F.W. Leuven}
\author[~~1~~4]{Wout M. Van Dijk}
\author[~~2~~5]{Yasuyuki Shimizu}
\author[1]{Maarten G. Kleinhans}
\affil[1]{\small Faculty of Geosciences, Utrecht University, Princetonlaan 8A, 3584 CB, Utrecht, The Netherlands}
\affil[2]{\small Royal HaskoningDHV, Rivers \& Coasts | Water, P.O. Box 151, 6500 AD Nijmegen, The Netherlands}
\affil[3]{\small Department of Environmental Sciences, Wageningen University, 6708 PB Wageningen, The Netherlands}
\affil[4]{\small Arcadis, Rivers \& Coasts, P.O. Box 220, 3800 AE Amersfoort, The Netherlands}
\affil[~~2~~5]{\small Faculty of Engineering, Hokkaido University, North 13, West 8, Kitaku, Sapporo, Hokkaido, 080-8628, Japan}

\runningtitle{Hydrodynamic modelling for physical scale experiments}
\runningauthor{Weisscher et al.}
\correspondence{Steven A.H. Weisscher (s.a.h.weisscher@uu.nl)}

%% These dates will be inserted by Copernicus Publications during the typesetting process.
\received{}
\pubdiscuss{} %% only important for two-stage journals
\revised{}
\accepted{}
\published{}

\firstpage{1}

\maketitle

\begin{abstract}
Physical scale experiments enhance our understanding of fluvial, tidal and coastal processes. However, it has proven challenging to acquire accurate and continuous data on water depth and flow velocity due to limitations of the measuring equipment and necessary simplifications during post-processing. A novel means to augment measurements is to numerically model flow over the experimental digital elevation models. We investigated to what extent the numerical hydrodynamic model Nays2D can reproduce unsteady, nonuniform shallow flow in scale experiments and under which conditions a model is preferred to measurements. To this end, we tested Nays2D for one tidal and two fluvial scale experiments and extended Nays2D to allow for flume tilting which is necessary to steer tidal flow. The modelled water depth and flow velocity closely resembled the measured data for locations where the quality of the measured data was most reliable, and model results may be improved by applying a spatially ~~variable~~varying roughness. The implication of the experimental data-model integration is that conducting experiments requires fewer measurements and less post-processing in a simple, affordable and labour-inexpensive manner that results in continuous spatio-temporal data of better overall quality. Also, this integration will aid experimental design.
\end{abstract}

%%
%%%%%%%%%% INTRODUCTION %%
%%
\section{Introduction}
Physical scale experiments greatly enhance our understanding of fluvial, estuarine and coastal processes and complement field observations and numerical models. The benefits of experiments that complement the other two means of research are twofold. Firstly, real material is used with its inherent laws and properties, as opposed to numerical models that require many parameters and approximations of laws for water flow, sediment transport
\citep[e.g.][]{MPM1948,VAnRijn2007I,Baar2019Nature} and lifeforms
\citep[e.g.][]{Baptist2007,Oorschot2016}. Secondly, experiments enable full control of the initial and boundary conditions and require little time to form entire systems, as opposed to the slow, ever-changing nature observed remotely or in the field.

~~However~~The focus of this study is on landscape scale experiments that simulate morphodynamics with shallow water depths of at maximum a few centimetres, i.e. in or just above the viscous sublayer. This kind of scale experiments differs from classical hydraulic flume studies \citep[e.g.][]{Struiksma1985,Nearyetal1999} and larger scaled experiments \citep[e.g.][]{Zanichellietal2004,Sivigliaetal2013} with water depths >10 cm in which flow data can be more easily measured with lasers and submerged flow meters (e.g. ADCP). In contrast, data collection in landscape experiments is often difficult, infrequent and hindered by various ~~practical~~ problems (~~Figure~~\Fig.~\ref{fig:intro}). ~~Here we focus on landscape scale experiments that siumulate biomorphodynamics with shallow water depths of a few centimetres.~~

Typical data collection in such experiments targets the following three elements: (1) the morphological development from overhead imagery and digital elevation models (DEMs) from laser scanning or stereo photography on a dry bed \citep[e.g.][]{Ashworth2004,HoyalSheets2009,Leduc2019}; (2) water depth estimated from dye and light attenuation, possibly combined with absolute water level point measurements \citep[e.g.][]{Peakall2007,TalPaola2007,TalPaola2010}, and; (3) flow velocity from particle imaging velocimetry on the water surface from floating particles or dye injections \citep[e.g.][]{Tambroni2005,Braudrick2009}. Due to the shallow water depths in landscape experiments, it is technically difficult to conduct flow measurements by submerged instruments without disturbance of the sediment transport and with the same spatial resolution as of the bathymetry. To overcome the drawbacks of data collection and post-processing, there has so far been one research team \citep{Tesser2007,Stefanon2010,Stefanon2012} that modelled water depth and flow velocity over DEMs of tidal basin scale experiments. However, the modelled data acquired by this novel method was not extensively validated against measured data and the model only applies for uniform flow conditions \citep{Marani2003}.

\begin{figure}[t!]
\centering
\includegraphics[width=10cm]{Fig01_Introduction.png}
\caption{Exemplary data of a physical scale experiment of a meandering river by \cite{VanDijk2013silt} show how data extraction may be distorted. (a) Overhead imagery shows cases of light overexposure and the distribution of white silica flour. The water is dyed red where the water colour saturation is a measure of water depth. Flow is from left to right. (b) Water levels, based on measured bed elevations and water depths estimated from water colour saturation, are too high above the floodplain ($z=0$~mm) at locations of abundant silica flour and too low at locations of overexposure.}
\label{fig:intro}
\end{figure}

Here we explore the possibility of extending the numerical flow model application by \cite{Tesser2007} and \cite{Stefanon2010,Stefanon2012} for unsteady, nonuniform flows in landscape scale experiments. ~~This will result in~~ We aim to complement the measured morphological data with continuous, spatio-temporally dense ~~model~~numerical data of ~~hydrodynamic parameters~~water depth, flow velocity and ~~sediment mobility that can be integrated with the experimental morphological data. This~~bed shear stress. On the one hand, this is a similar ~~to the~~ practice ~~of hydrodynamic~~to modelling ~~in~~flow over the measured morphology of real rivers and estuaries \citep[e.g.][]{Berends2019~~}. An~~}, whilst here the shallow water equations need to be solved. On the other hand, this practice differs from remodelling the morphological development of a scale experiment \citep[e.g.][]{Struiksma1985}, which are subject to all the combined errors of sediment transport predictors \citep{Baar2019Nature}. The extended integration of experimental

data and a numerical ~~flow~~ model would not only expand the possibilities for data analyses of ~~experiments~~a series of experiment bed scans, but would also open up fast methods of testing alternative experimental settings for either an experimental or idealised ~~DEM~~morphology. This would save valuable time in the laboratory, especially for long-lasting experiments that include vegetation \citep[e.g.][]{Braudrick2009,VanDijk2013veg,Lokhorst2019}.

~~The numerical model Nays2D, explained in Sect.~\ref{sec:methods}, was applied to two fluvial experiments and one tidal scale experiment that are representative of other river flume setups with uni-directional flow \citep[e.g.][]{Ashmore1991a,TalPaola2010,Braudrick2009} and for estuary flume setups with reversing flow \citep[e.g.][]{Reynolds1889,Tambroni2005,Braat2018}. Below, a brief review is given on the main findings and general setup of the selected experiments, as well as on the measuring and post-processing techniques used in scale experiment studies.~~

%%
%%%%%%%%% REVIEW %%%%%%%%%%%%%%%%%%%%%%%%%%%%%%%%%%%%%%
%%
\section{Review: Experimental Data Collection and Post-Processing Techniques} \label{sec:review}}

~~}.}~~
~~\subsection{Scale Experiments}~~
~~The fluvial experiments in the Eurotank flume by \citet{VanDijk2013silt} demonstrated the importance of cohesive floodplain formation for replicating a meandering channel in a physical scale-experiment. Floodplain formation by the deposition of fines was found to be sufficient to maintaining a sinuous, single-thread channel in the absence of vegetation. In contrast, a weakly braided river pattern developed in the control experiment without fines. Fines were represented by white, silt-sized silica flour that was added to the river discharge. Additionally, regular floods were applied to the river discharge to enhance the deposition of cohesive deposits on the floodplain, and the inflow was periodically perturbed to maintain meandering dynamics \citep{LanzoniSeminara2006,VanDijk2012,Weisscher2019Meander}. The collected data constitutes overhead imagery and DEMs from line-laser altimetry. In parallel, floodplain has been formed experimentally with vegetation \citep{TalPaola2010,Braudrick2009}, but this requires parameterisation of vegetation that, although possible \citep{Baptist2007,Weisscher2019Meander}, introduces uncertainties that would hamper model-data comparison for this study.~~

~~The tidal experiment in the Metronome flume by \citet{Leuven2018} showed the development of an entire estuary with erodible boundaries and self-formed bars on a laboratory scale. The self-formed estuary planform was characterised by along-channel alternations of shallow, wide sections that accommodated large bars, and deep bottlenecks where the main confluences were found. The Metronome flume tilts over the short central axis (Fig.~\ref{fig:metronome}), which differs from previous stationary flume setups with sea level fluctuations \citep{Reynolds1889,Reynolds1891,MayorMora1997,Tambroni2005,Tesser2007,Stefanon2010,Stefanon2012,VlaswinkelCantelli2011,Iwasaki2013}. This tilting motion steers flows in both the flood and ebb direction that are strong enough to move sediment \citep{Kleinhans2017tide}. The collected data constitutes overhead imagery, DEMs from stereo-photography and flow measurements by large-scale particle imaging velocimetry (PIV) over a tidal cycle. Earlier experiments had tidal flow driven by slow sea level fluctuations, which is closer to the cause of tidal currents in nature but leads to lower sediment mobility \citep[e.g.][]{Tambroni2005,Stefanon2010}. Moreover, such flows can be modelled with simpler flow models \citep{Marani2003,Stefanon2010} that provide a less rigorous test of the numerical model applied here.~~

\begin{table}[t]
\caption{Data collection techniques in fluvial and tidal scale experiments with erodible boundaries and flows shallower than a few centimetres. `Overhead imagery' constitutes imagery or video from a camera at a fixed position that potentially allows for the classification of the experiment planform. Water depths `est. from physics' are determined for a few cross-sections assuming uniform flow and a given discharge. `SfM' is structure-from-motion photogrammetry. The field `Remarks' contains additional sediments/vegetation on top of the main sediment that may interfere with overhead imagery analyses.}
\resizebox{\textwidth}{!}{%
\begin{tabular}{llllllll}
\hline
\multirow{2}{*}{Paper} & \multirow{2}{*}{Type of experiment} &
\multicolumn{5}{c}{Measurements} & \multirow{2}{*}{Remarks} \\ \cline{3-7}
 & & \textit{\begin{tabular}[c]{@{}l@{}}Overhead\\ imagery\end{tabular}} & \textit{Elevation} &
\textit{DEM} & \textit{Water depth} & \textit{\begin{tabular}[c]{@{}l@{}}Flow\\
velocity\end{tabular}} & \\ \hline
\textit{unidirectional flow} & & & & & & & \\
\citet{Friedkin1945} & meandering/braided river & x & point gauge & x & point gauge & - & silt, coal, loess \\
\citet{SchummKhan1972} & alternating bars & - & point gauge & - & point gauge & - & kaolinite \\
\citet{Schumm1987} & alluvial fan & x & burial of pins & - & - & - & - \\
\citet{Ashmore1991a,Ashmore1991b} & braided river & x & point gauge & - & point gauge & - & - \\
\citet{Ashworth1994} & braided river & x & point gauge & - & point gauge & - & - \\
\citet{GranPaola2001} & braided river & x & laser/point gauge & x & water colour & PIV & vegetation \\
\citet{Ashworth2004} & braided river & x & laser & x & - & - & - \\
\citet{Peakall2007} & braided river & x & point gauge & - & point gauge & PIV & - \\
\citet{TalPaola2007,TalPaola2010} & meandering river & x & laser & - & water colour & - & vegetation \\
\citet{HoyalSheets2009} & alluvial fan & x & ultrasound & x & est. from physics & dye & - \\
\citet{VanDijk2009} & alluvial fan & x & SfM & x & est. from physics & - & - \\
\citet{Braudrick2009} & meandering river & x & laser & x & point gauge & dye & vegetation \\
\citet{Gardner2011} & braided river & x & SfM & x & - & - & - \\
\citet{VanDijk2012,VanDijk2013silt} & meandering/braided river & x & laser & x & water colour & - & silica flour \\
\citet{VanDijk2013veg} & meandering river & x & laser & x & water colour & - & vegetation \\
\citet{Lageweg2013,Lageweg2014} & meandering river & x & laser & x & water colour & - & silica flour \\
\citet{Leduc2019} & braided river & x & SfM & x & SfM & - & - \\
 & & & & & & & \\
\textit{reversing flow} & & & & & & & \\
\citet{Reynolds1889,Reynolds1891} & estuary/tidal basin & - & contour-line & x & - & - & - \\
\citet{MayorMora1997} & tidal channel & x & point gauge & - & point gauge & - & - \\
\citet{Tambroni2005} & tidal channel & - & ultrasound & x & ultrasound & PIV & - \\
\citet{Tesser2007} & tidal basin & - & laser & x & ultrasound & model & - \\
\citet{Stefanon2010,Stefanon2012} & tidal basin & - & laser & x & ultrasound & model & - \\
\citet{VlaswinkelCantelli2011} & tidal basin & x & laser & x & bathymetry & - & - \\
\citet{Kleinhans2012,Kleinhans2015b_tide} & tidal basin & x & x & - & - & water colour & PIV & - \\
\citet{Iwasaki2013} & tidal basin & x & x & \textit{unclear} & - & - & - & - \\
\citet{Kleinhans2014Tide} & tidal channel & x & zSnapper^{\textregistered} & x & water colour & - & - \\

\citet{Braat2018} & estuary & x & SfM & x & water colour & PIV & walnut shell \\
\citet{Leuven2018} & estuary & x & SfM & x & - & PIV & - \\
\citet{Leuven2019} & tidal channel & x & SfM & x & water colour & PIV & - \\ \hline
\end{tabular}%
}
\label{tab:exp_measurements}
\end{table}

~~%%%~~
~~\subsection{Experimental Data Collection and Post-Processing Techniques}~~
In order to quantify the hydro- and morphodynamics of a ~~flume~~landscape scale experiment with shallow flow, the following three data types are commonly measured: dry bed elevation, water depth and flow velocity (Table~\ref{tab:exp_measurements}). Below, the data collection and post-processing methods of these data are presented in conjunction with their drawbacks and achievable level of accuracy.

Firstly, bed elevation of experiments can be acquired through numerous techniques. These include a water level contour survey \citep{Reynolds1889,Reynolds1891}, a manual/digital point gauge survey \citep[e.g.][]{Friedkin1945,Peakall2007}, 3D/laser and structured light (zSnapper^{\textregistered}) scanning \citep[e.g.][]{GranPaola2001,Tambroni2005,Lageweg2014,Kleinhans2014Tide,Marra2014}, ultrasonic echosounding \citep[e.g.][]{BestAshworth1994,HoyalSheets2009,Stefanon2010,Stefanon2012}, and structure-from-motion (SfM) photogrammetry through which photos are geo-referenced to ground control points (Agisoft PhotoScan) \citep[e.g.][]{Westoby2012SfM,Leduc2019}. The most accurate technique is the point gauge survey ($\pm$~0.1~mm) \citep{BestAshworth1994}, which does not require the flume to be drained. However, point gauging is terribly slow to get full coverage, as is the case for the water level contour survey, in which dry bed-water boundaries are registered for different water levels \citep{Reynolds1889,Reynolds1891}. In contrast, scanning, sounding and photogrammetry are much quicker and typically result in a vertical accuracy of $\pm$~0.5 to 1~mm \citep{Peakall2007,Leduc2019}. Yet, these three techniques require a dry bed, apart from a few kinds of laser scanners \citep{Tesser2007,Stefanon2010,Stefanon2012}. Consequently, the bed may be disrupted during the draining and refilling of the flume. Also, vegetation hampers their accurate reading of the bed elevation \citep[e.g.][]{GranPaola2001}. In consequence of these drawbacks, the number of DEMs is usually limited.

Secondly, water depth maps are acquired while the experiment runs in either of two approaches: water depth is derived from the dyed water colour saturation, or from measured water levels. As for the first approach on dye, the water colour saturation is an indicator of water depth that is recorded by overhead cameras \citep[e.g.][]{Carbonneau2006,TalPaola2007,TalPaola2010}. To augment differences in colour saturation, some studies \citep[e.g.][]{VanDijk2013silt,Leuven2019} converted the overhead RGB imagery to the CIE L*a*b* colour space; L* is a scale for luminosity, a* is a scale from green to red, and b* is a scale from blue to yellow. For calibration, the bed elevation of a map or transect is related to the corresponding values of colour saturation, after which a regression is used to convert the overhead imagery to water depth maps. Ideally, a regression is used that captures the exponential saturation of water colour with increasing water depth \citep{Carbonneau2006}. A high accuracy up to 1~mm is mentioned in literature \citep{TalPaola2007,TalPaola2010}, but may be much lower for substrates with mixed sediments with different colours and for lighting variations (Figure~\ref{fig:intro}) \citep[e.g.][]{VanDijk2013silt}.

Alternatively, water depth is readily derived from water levels and bed elevations. Water levels are recorded as point measurements using an ultrasonic echosounder or water level gauge \citep[e.g.][]{MayorMora1997,Tambroni2005} or are derived from SfM photogrammetry \citep{Leduc2019}. Although sounding and gauging ~~is~~are more time-consuming to get full coverage, the data has a much smaller claimed error of 0.2~mm \citep{Tambroni2005}. As for SfM photogrammetry, this only works up to present for unidirectional flow with rigorous calibration and has a vertical accuracy of 1~mm \citep{Leduc2019}. Additionally, few studies estimate water depth along cross-sections of the known bathymetry from uniform flow and an estimated discharge \citep{HoyalSheets2009,VanDijk2009,VlaswinkelCantelli2011}.

Thirdly, flow velocity maps are created by tracking floating particles \citep{Peakall2007,Kleinhans2017tide}, soap bubbles \citep{GranPaola2001} and dye \citep{HoyalSheets2009,Braudrick2009} with overhead cameras. Either the data are partly manually digitised or a technique is used called particle imaging velocimetry (PIV) \citep[e.g.][]{MoriChang2003}. Herein, small floating particles are seeded on the water surface, and their positions are recorded at a high frequency by overhead cameras. Subsequently, surface flow velocity and direction are computed by tracking the displacement of the particles from pairs of consecutive images. However, this technique falls flat for regions with either sparse or superabundant particles where it is infeasible either to get sufficient coverage or to track individual particles. Also, PIV particles may become stranded on bars, which culminates in much lower or absent measured flow velocities that are especially troublesome in tidal experiments \citep{Leuven2018}. Another drawback is that the PIV particle removal is done by increasing the water depth and drain the flume, which may disrupt the bed. For this reason, PIV measurements cannot be done in experiments with vegetation and light-weight material, for the latter would be uprooted or displaced. This issue may be overcome by using soap bubbles \citep{GranPaola2001}. The error of PIV measurements of mean flow velocities may be as small as 0.5 pixel size if particle size and density are chosen correctly \citep{Weitbrecht2002}. Finally, measuring flow in the water column is infeasible with the available equipment reported in literature; this is due to the shallow water depth of at most a few cm in the type of physical scale experiments discussed here.

Thus far, only one research group has used a numerical model to create flow velocity maps for scale experiments with shallow flow \citep{Tesser2007,Stefanon2010,Stefanon2012}. They used a tidal basin DEM and the boundary conditions as input and solved the Poisson boundary value problem, which is valid for systems where the water surface can be assumed horizontal \citep{Marani2003}. This resulted in maps of depth-averaged flow velocities over a tidal cycle. Although the model had been validated for the Venice Lagoon \citep[e.g.][]{Defina2000}, the model was not calibrated for the experiment due to a lack of flow velocity measurements.

%%
\begin{figure}[b!]
\includegraphics[width=14cm]{EurotankMetronome.png}
\caption{The flume setups of the two scale experiments tested in this study. (a) The Eurotank flume was used to simulate meandering and braided rivers in parallel on the left and right part of the flume, respectively \citep{VanDijk2013silt}. Water colour was converted to blue for visual comparison with (b) the second scale experiment in the tilting flume the Metronome that was used to simulate estuaries \citep{Leuven2018}. The flume is tilted over the short central axis, which steers flood and ebb flows that favour ample sediment transport in both tidal directions.}
\label{fig:metronome}
\end{figure}

%%%
%%%%%%%%%% METHODOLOGY %%%%%%%%%%%%%%%%%%%%%%%%%%%%
%%%
\section{Methods} \label{sec:methods}
\subsection{Selected Scale Experiments}
Two fluvial experiments and one tidal experiment were selected for testing that are representative of other river flume setups with uni-directional flow \citep[e.g.][]{Ashmore1991a,TalPaola2010,Braudrick2009} and for estuary flume setups with reversing flow \citep[e.g.][]{Reynolds1889,Tambroni2005,Braat2018}. Below, a brief review is given on the main findings and general setup of the selected experiments.

The fluvial experiments in the Eurotank flume by \citet{VanDijk2013silt} demonstrated the importance of cohesive floodplain formation for replicating a meandering channel in a physical scale-experiment. Floodplain formation by the deposition of fines was found to be sufficient to maintaining a sinuous, single-thread channel in the absence of vegetation. In contrast, a weakly braided river pattern developed in the control experiment without fines. Fines were represented by white, silt-sized silica flour that was added to the river discharge. Additionally, regular floods were applied to the river discharge to enhance the deposition of cohesive deposits on the floodplain, and the inflow was periodically perturbed to maintain meandering dynamics \citep{LanzoniSeminara2006,VanDijk2012,Weisscher2019Meander}. The collected data constitutes overhead imagery and DEMs from line-laser altimetry. In parallel, floodplain has been formed experimentally with vegetation \citep{TalPaola2010,Braudrick2009}, but this requires parameterisation of vegetation that, although possible \citep{Baptist2007,Weisscher2019Meander}, introduces uncertainties that would hamper model-data comparison for this study.

The tidal experiment in the Metronome flume by \citet{Leuven2018} showed the development of an entire estuary with erodible boundaries and self-formed bars on a laboratory scale. The self-formed estuary planform was characterised by along-channel alternations of shallow, wide sections that accommodated large bars, and deep bottlenecks where the main confluences were found. The Metronome flume tilts over the short central axis (Fig.~\ref{fig:metronome}), which differs from previous stationary flume setups with sea level fluctuations \citep{Reynolds1889,Reynolds1891,MayorMora1997,Tambroni2005,Tesser2007,Stefanon2010,Stefanon2012,VlaswinkelCantelli2011,Iwasaki2013}. The tilting motion periodically generates a slope in the landward direction during flood and a slope in the seaward direction during ebb, which result in tidal currents strong enough to move sediment along the entire estuary \citep{Kleinhans2017tide} (Supplementary movie). The collected data constitutes overhead imagery, DEMs from stereo-photography and flow measurements by large-scale particle imaging velocimetry (PIV) over a tidal cycle. Earlier experiments had tidal flow driven by slow sea level fluctuations, which is closer to the cause of tidal currents in nature but leads to lower sediment mobility \citep[e.g.][]{Tambroni2005,Stefanon2010}. Moreover, such flows can be modelled with simpler flow models \citep{Marani2003,Stefanon2010} that provide a less rigorous test of the numerical model applied here.

\subsection{Numerical Model Nays2D}
The numerical model Nays2D was selected to simulate water flow of fluvial and tidal landscape scale experiments for the following reasons. Firstly, Nays2D is one of few models (as opposed to e.g. Delft3D) that accountsthat can account for shallow flow of at maximum a few centimetres deep. This is opposed to more common models for the simulation of large-scale fluvial and tidal morphodynamics (e.g. Delft3D) that often have build-in thresholds for minimum water depths. Secondly, Nays2D is open source (as opposed to e.g. FLOW-3D), so the technique tested in this study is freely available for third parties.

Nays2D solves the depth-averaged nonlinear shallow water equations, given by the following three equations in Cartesian coordinates, in which Eq.~(\ref{eq:hydro1}) is the preservation of mass and Eq.~(\ref{eq:hydro2}-\ref{eq:hydro3}) are the preservation of momentum in the streamwise and transverse direction, respectively:

\begin{equation} \label{eq:hydro1}
\frac{\partial h}{\partial t} + \frac{\partial (h\bar{u})}{\partial x} + \frac{\partial (h\bar{v})}{\partial y} = 0
\end{equation}

\begin{equation} \label{eq:hydro2}
\frac{\partial \bar{u}}{\partial t} + \bar{u}\frac{\partial \bar{u}}{\partial x} + \bar{v}\frac{\partial \bar{u}}{\partial y} + g\frac{\partial H}{\partial x} + \frac{g\bar{u}\sqrt{\bar{u}^2+\bar{v}^2}}{C^2h} - \nu_t\left(\frac{\partial^2\bar{u}}{\partial x^2}+\frac{\partial^2\bar{u}}{\partial y^2}\right) = 0
\end{equation}

\begin{equation} \label{eq:hydro3}
\frac{\partial \bar{v}}{\partial t} + \bar{u}\frac{\partial \bar{v}}{\partial x} + \bar{v}\frac{\partial \bar{v}}{\partial y} + g\frac{\partial H}{\partial y} + \frac{g\bar{v}\sqrt{\bar{u}^2+\bar{v}^2}}{C^2h} - \nu_t\left(\frac{\partial^2\bar{v}}{\partial x^2}+\frac{\partial^2\bar{v}}{\partial y^2}\right) = 0
\end{equation}

in which t is time (\unit{s}), $\bar{u}$ and $\bar{v}$ are the depth-averaged flow velocity (\unit{m~s^{-1}}) in the streamwise (x) and transverse (y) direction, H is the water level (\unit{m}), h is the water depth (\unit{m}), C is the Chezy roughness (\unit{m^{0.5}~s^{-1}}), g is the acceleration due to Earth's gravity (\unit{m~s^{-2}}) and ~~v~~ν_t is the eddy viscosity coefficient (\unit{-}). Eddy viscosity is approximated as

\begin{equation} \label{eq:eddy_visc}
~~v~~\nu_t = \frac{\kappa}{6}au_*h+b
\end{equation}

% where κ is the von Karman constant (-), u_* is the shear velocity (\unit{m~s^{-1}}), and a and b are user-defined constants set to the default values of 1 and 0, respectively. u_* is given as

\begin{equation} \label{eq:u_star}
u_{*,x} = \sqrt{\frac{g\bar{u}\sqrt{\bar{u}^2+\bar{v}^2}}{C^2}} \hspace{5mm}\&\hspace{5mm} u_{*,y} = \sqrt{\frac{g\bar{v}\sqrt{\bar{u}^2+\bar{v}^2}}{C^2}}
\end{equation}

in which $u_{*,x}$ and $u_{*,y}$ are the streamwise and transverse components of the shear velocity (\unit{m~s^{-1}}).

The hydrodynamics were solved by dividing each time step into two parts, namely an advective part that was solved using a cubic-interpolated pseudoparticle (CIP) method, and a nonadvective part that was solved with a conventional finite difference method \citep{Yabe1990}. Since the aim of this study is to complement bathymetric data with hydrodynamic data rather than to reproduce the experiment, sediment transport and morphological updates were disregarded.

\begin{figure}[t!]
\includegraphics[width=15cm]{Flowchart8.pdf}
\centering
\caption{Workflow of integrating physical scale experiments and the numerical hydrodynamic model Nays2D to acquire water depth, flow velocity and sediment mobility maps (i.e., excluding point measurements). The DEM and corresponding boundary conditions are input to the model. Grey elements apply only to tilting flume experiments that simulate tidal systems. End products are on the bottom row and are indicators of hydrodynamics and morphological change.}
\label{fig:flowchart}

\end{figure}

Input to Nays2D comprised a DEM of each experiment as initial condition and the corresponding boundary conditions (Fig.~\ref{fig:flowchart}; Table~\ref{tab:boundaryconditions_rivers}). For the river modelling, the two DEMs (meandering and braided rivers) corresponded to the final flood stage; a constant bankfull discharge of 0.5~\unit{L~s^{-1}} entered at the upstream boundary, and the water level at the downstream boundary was derived from uniform flow. For the estuary modelling, the DEM was used that corresponded to tidal cycle number 5887 \citep[see][]{Leuven2018}, and a 0.1~\unit{L~s^{-1}} river discharge entered only during the ebb phase; DEMs at later stages could not be used since the ebb-tidal delta was incomplete due to the overhanging wave generator. The estuary DEM was interpolated to a coarser rectangular grid with 2.5$\times$2.5~\unit{cm} grid cells to limit model ~~runtime~~run time to at maximum one day. In agreement with modelling practices for natural systems \citep{Arcement1989}, a spatially uniform Manning roughness coefficient of 0.02~\unit{s~m^{1/6}} was applied of which the sensitivity will be assessed later. The reason for not using a spatially variable friction, which could be computed from maps of grain size, is that such maps would currently include all measurement errors due to lighting and sediment colour. If these errors are significantly reduced in future studies, spatially varying friction maps are a viable option. The model was cold started with an initial water slope equal to the valley slope of the DEM with initial flow velocities calculated from uniform flow.

Nays2D was extended to enable periodical tilting of the estuary DEM and the downstream water level boundary to drive tidal flow similar to the tilting flume the Metronome (Fig.~\ref{fig:metronome}). The domain was tilted sinusoidally with a period of 40~s and an amplitude of 0.075~\unit{m}, meaning a maximum gradient of 0.0075~\unit{m~m^{-1}}. In the Metronome, the water level at the downstream boundary was set by a weir that moved in counterphase to the flume tilting so as to maintain a constant sea level of +0.065~m during tilting \citep[see][for explanation]{Kleinhans2017tide,Leuven2018}. As the experiment progressed, the weir amplitude was gradually reduced with the reduction of the length of the open sea due to the development of the large ebb-tidal delta; at tidal cycle number 5887, the weir had an amplitude of 0.004~\unit{m}. To mimic the action of the weir in the model Nays2D, a sine function was imposed on the water depth at the downstream boundary, and the sea around the ebb-tidal delta was assigned a high diffusivity of $b=0.02$ for numerical stability.

%%
\subsection{Data Analysis}
Maps of water depth and flow velocity were compared to the measured data. For the two rivers, only water depth was compared, as flow velocity was not systematically measured other than sparse estimates of mid-channel flow (see Fig.~S1 for modelled flow velocity maps). To explore the causes of the water depth differences between the model and the experiments, the river planforms were classified into six classes (Fig.~S2). The first two classes comprised the locations of white silica flour and overhead light overexposure, which were based on the overhead imagery. The remaining four classes were morphological units with increasing levels of inundation, from a soaked bed with negligible water depth to a channel. These units were based on modelled flow, for which we used bed elevation times flow velocity to the power three that proved well to separate transporting channels from inactive ones \citep{Weisscher2019Meander}.

\begin{table}[t!]
  \caption{Model settings and boundary conditions of the physical scale experiments in Nays2D. The first block of parameters is retrieved from the experiments, the second block is user-defined.}
  \begin{tabular}{llrr}
  \hline

```
    \begin{tabular}{r} Parameter\\hfill \end{tabular} &
    \begin{tabular}{r} Unit\\hfill \end{tabular} &
    \begin{tabular}{r} \citet{VanDijk2013silt}\\\textit{meandering/braided rivers} \end{tabular}
    & \begin{tabular}{r} \citet{Leuven2018}\\\textit{estuary} \end{tabular} \\ \hline
    River discharge             & \unit{L~s^{-1}} & 0.5 & 0.1\\
    Grain size $\mathrm{d_{50}}$  & \unit{m} & 0.51$\times$10$^{-3}$ & 0.55$\times$10$^{-3}$ \\
    Downstream water level       & \unit{m} & \textit{uniform flow} & 0.065\\
    Tilting period (flume \& weir)& \unit{s} & | & 40 \\
    Tilting amplitude (flume)     & \unit{m} & | & 0.075\\
    Tilting amplitude (weir)      & \unit{m} & | & 0.004\\
    \\
    Time step                   & \unit{s} & 0.02 & 0.005 \\
    Manning's n                 & \unit{s~m^{1/6}} & 0.02 & 0.02 \\\hline
    \end{tabular}
    \label{tab:boundaryconditions_rivers}
\end{table}
```

Maximum and minimum water depths in the estuary experiment were compared to bracket the tidal conditions. The 16~overhead images taken during the tidal cycle were converted into measured water depth maps. To account for incoming light from a window at the seaward side of the flume, two conversions were formulated for the upstream and downstream boundaries that were linearly interpolated along the flume. The equation for the upstream boundary was $h = 1.43.10^{-7}\times Blueness^{-15.68}+0.004$ and for the downstream boundary was $h = 2.41.10^{-2}\times Blueness^{-2.19}+0.092$, where $Blueness$ is the b* band in the CIE L*a*b* colour space.

Surface flow velocity measurements of the estuary experiment were compared with modelled depth-averaged velocities. To this end, the modelled flow velocities were converted to surface flow velocity using

```
\begin{equation} \label{eq:depthprofile}
    u_z = \frac{u_*}{\kappa} ln\left( \frac{z}{z_0} \right)
\end{equation}
```

in which u_z is the flow velocity (\unit{m~s^{-1}}) at depth z (\unit{m}), with depth-averaged flow velocity at $0.36~h$, and z_0 is the zero-velocity level for rough flow (\unit{m}). Modelled depth-averaged flow velocity and shear velocity were used to calculate z_0, from which u_z was calculated at the water surface. Grid cells lacking one or more of the 16~PIV measurements during the tidal cycle were filtered out to enable a fair comparison of experimental data and model throughout the entire tidal cycle. The comparison focused on morphologically relevant variables; these include the tidal flow velocity maxima during the ebb and flood phases, which are important for sand transport \citep{Friedrichs2011}, and the tidally averaged residual flows, which are important for mud transport \citep{Postma1961,Groen1967}.

%%%
%quantification of model accuracy
Finally, the sensitivity to the Manning roughness coefficient was tested for the range $0.016 - 0.024$~\unit{s~m^{1/6}} that agrees with common coefficients for sand \citep{Arcement1989}. The mean absolute error (MAE) and mean bias error (MBA) quantify the difference between the model and the measurements. The MAE is ~~computes~~computed as the average of absolute differences between the modelled and measured data. The MBA is computed as the average difference to quantify how much the model over- or underpredicts the measured data.

%%%
%%%%%%%%%% RESULTS %%%%%%%%%%%%%%%%%%%%%%%%%%%%%%%%%%%
%%%
\section{Results}
\subsection{Meandering and Braided Rivers}
\subsubsection{Water Depth}
The modelled water depth resembles the measured data for both river types for locations where the quality of the experimental data is good (Figs.~\ref{fig:WaterDepthComp}a-f,~\ref{fig:ScatterClasses}a-d,~S2). Similar to the meandering river experiment, the model produces a single sinuous channel with swale channels and significant overbank flow. The flowflow that is clearly focused in a single mainsinuous channel, especially for $x>4$~\unit{$~m}, which is (Fig.~S1), despite the same domain range in which swale channels are present on the inner bendsmulti-channel character of the meandering channel (Fig.~\ref{fig:WaterDepthComp}b).DEM and the considerable overbank flow. This distinction of a main sinuous channel and swale channels is less distinct in the model for $x<4$~\unit{m}. This is also the domain range with slightly more modelled overbank flow over the floodplain compared to the experiment (Fig.~\ref{fig:WaterDepthComp}c). The mean absolute error is small, albeit larger for the channels (MAE~$=1.73$~\unit{mm}) than the low/high inundated areas (MAE $=0.81$~\unit{mm}), and the model bias error is negligible (MBE~$<0.1\cdot$~MAE) (Fig.~\ref{fig:ScatterClasses}a,b), given a maximum water depth of 20~\unit{mm}.

\begin{figure}
\centering
\includegraphics[width=12.5cm]{Fig03_WaterDepthComparison_v8.png}
\caption{Measured and modelled water depth (a-c) for the meandering and (d-f) braided rivers by \cite{VanDijk2013silt} and (g-l) for the estuary by \cite{Leuven2018}. In case of the estuary, panels (g-i) show the maximum water depth during a tidal cycle, and panels (j-k) show the minimum water depth during a tidal cycle. Maps of difference are determined by subtraction of modelled from measured water depth.}
\label{fig:WaterDepthComp}
\end{figure}

The braided river model reproduces the division of flow over about two channels with little overbank flow (Fig.~\ref{fig:WaterDepthComp}d-f). However, the model predicts slightly more water flowing through the secondary channels and less through the main channel (for example the secondary channel around $x=6$~\unit{m}, $y=1$~\unit{m} in Fig.~\ref{fig:WaterDepthComp}f). Overall, the model error is slightly larger than of the meandering river, with an MAE~$=2.31$~\unit{mm} and MBE~$=-0.65$~\unit{mm} for channels and an MAE~$=1.30$~\unit{mm} and MBE~$=-0.25$~\unit{mm} for low/high inundated areas (Fig.~\ref{fig:ScatterClasses}b,d); the bias errors indicate that modelled water depths are on average lower than the measured values for the braided river.

The modelled flow is more reliable at locations with abundant white silica flour where the measured data are quite inaccurate (Figs.~\ref{fig:intro}b,~S2c). It is at these locations that the measured water levels, calculated as water depth from water colour added on the bathymetry, are unrealistically high above the surrounding floodplain. The reason for such large measured water depths for the upper meandering river (Fig.~\ref{fig:WaterDepthComp}a-c) is that the white silica flour enhanced the colour contrast with respect to the yellowish sandy substrate. In consequence, higher redness values were recorded for floured regions on the a* band that \citet{VanDijk2013silt} used to estimate water depths. However, as this effect was unaccounted for during post-processing, too large water depths were assigned to these 'redder' areas.

\begin{figure}[t!]
\centering
\includegraphics[width=12.5cm]{Figxx_ScatterClasses_WaterDepth.png}
\caption{Comparison between measured and modelled water depths for different classes for the (a,c) meandering and (b,d) braided rivers, as well as for the (e) maximum and (f) minimum water depths in the estuary. The scatter density plots exclude floodplain and erroneous measured data (e.g. due to white silica flour), which are included in Figs.~S2 (rivers) and S3 (estuary). Colours indicate the occurrence frequency.}
\label{fig:ScatterClasses}
\end{figure}

%%
\subsection{Estuary}
\subsubsection{Water Depth}
Periodic tilting of the estuary DEM that mimicked the motion of the tilting flume adequately reproduced the propagating behaviour of the tidal wave (Supplementary movie). Moreover, the modelled tidal wave caused maximum and minimum water depths close to those observed with an MAE~$=1.96$~\unit{mm} for maximum water depths and an MAE~$=2.64$~\unit{mm} for minimum water depths (Figs.~\ref{fig:WaterDepthComp}g-l,~\ref{fig:ScatterClasses}e,f,~S3,~S4). These errors are small compared to the largest water depths recorded in the estuary of about 35~\unit{mm}.

Overprediction by the model mainly occurs at the ebb-tidal delta ($x>18$~\unit{m} in Fig.~\ref{fig:WaterDepthComp}i,l). This is predominantly due to the difference of the downstream boundary conditions between the experiment and the model. In particular, the amount of water entering the flume during flood was somewhat limited by the pumping capacity in the experiment. In contrast, the influx of water in the model was determined with a uniform flow assumption, causing larger inflow that increased the water depths on the ebb-tidal delta. In turn, this larger influx likely contributed to the slightly larger maximum modelled water depths especially in the downstream half of the estuary.

Underprediction by the model is primarily ascribed to two factors, namely the chosen hydraulic roughness coefficient (model-based) and the water depth conversion from colour saturation (experimental data-based). Firstly, the observations clearly show that the tidal wave propagated faster in the deeper channels than over the shallow bars, causing flow to curl around bars (Supplementary movie). In the model, however, the partitioning of flow between channels and bars is less asymmetrical. In consequence, flood-dominant channels that end in a shoal may receive more modelled inflow over their shoal during ebb, resulting in overall slightly larger water depths (e.g. the red tidal channel at $x=8$~\unit{m} in Fig.~\ref{fig:WaterDepthComp}l). This implies that the model diffusivity and/or hydraulic roughness on the bars are too small. Secondly, the experimental data-model comparison is sensitive to the water depth conversions, which are less accurate for shallow water depths (Figs.~\ref{fig:ScatterClasses}f). Specifically, the nonlinear conversion equations used in this study and by \citet{Leuven2018} overpredict water depths for very shallow flow (i.e., $h<5$~\unit{mm}; Fig.~\ref{fig:ScatterClasses}f)) so as to get the deeper water depths right. Therefore, measured water depths of very shallow flow over bars are too large, which explains most of the differences between model and experimental data for minimum water depths.

\begin{figure}[b!]
\centering
\includegraphics[width=12.5cm]{Figxx_EstuaryFlow_manning020_norm_v9.png}

\caption{(b-d) Maximum ebb and (e-g) flood flow velocity with (a) the estuary morphology for reference. Maps of difference are determined by subtraction of modelled from measured surface flow velocity. `X' and `O' in (a) are the locations at which tidal stage diagrams were made in Fig.~\ref{fig:FlowDepthDiagram} of channels and shoals, respectively.}
\label{fig:FlowComp}
\end{figure}

\begin{figure}[t!]
\centering
\includegraphics[width=15cm]{Figxx_SurfaceFlowPhases_v6.png}
\caption{(a) Surface flow velocity along the estuary, given as the $\mathrm{90^{th}}$ percentile of the streamwise flow velocity component. (b) The effect of Manning on the surface flow velocity and (c) the phase-dependent median water level of each cross-section along the estuary. Colours indicate the phase in the tidal cycle.}
\label{fig:SurfaceFlow}
\end{figure}

\begin{figure}[t!]
\centering
\includegraphics[width=12.5cm]{Figxx_FlowDepthDiagrams_v6.png}
\caption{Tidal stage diagrams showing water depth versus surface flow velocity for a channel and shoal at (a) $x=14.6$~\unit{m} and (b) $x=10.8$~\unit{m} in Fig.~\ref{fig:FlowComp}a. Water depth and surface flow velocity were averaged for a 5x5 cell window. Colours indicate the phase in the tidal cycle.}
\label{fig:FlowDepthDiagram}
\end{figure}

\begin{figure}[t!]
\centering
\includegraphics[width=12.5cm]{Fig06_ResidualFlow_manning020_surf_v6.png}
\caption{Residual surface flow velocity maps show similar spatial flow patterns and magnitudes between (a) the measured data and (b) model output, apart from the upstream 6~m. This upstream region was underseeded with PIV particles, which resulted in wrongly measured flow velocities. Therefore, computation of the mean absolute/bias errors was done for $x>6$~\unit{m}.}
\label{fig:ResidualFlow}
\end{figure}

%%
\subsubsection{Ebb and Flood Flow}
The modelled spatial pattern of peak flow velocities resembles that of the PIV measurements (Fig.~\ref{fig:FlowComp}). Both model and measurements show that peak ebb and flood flow are relatively large in channels and around bottlenecks, while they are relatively small on bars and in wider sections of the estuary. Furthermore, peak flow velocities decrease in the landward direction from $\pm$~40~\unit{cm~s^{-1}} at the estuary mouth to $\pm$~30~\unit{cm~s^{-1}} at $x=2$~\unit{m} (Fig.~\ref{fig:SurfaceFlow}a,b). Over the entire tidal cycle, the model has a small MAE~$=6.45$~\unit{cm~s^{-1}}, which is about 1/7 of the maximum surface flow velocity; in other words, the modelled order of magnitude is close to the measurements'. Also, a different manning roughness results in fairly similar water levels and flow velocities along the estuary, with slightly smaller flow velocities and water level variations for a higher roughness (Fig.~\ref{fig:SurfaceFlow}b,c).

The model has full spatial cover, while experimental data are lacking particularly near the estuary mouth and for the shallower areas (Fig.~\ref{fig:FlowComp}a,b,e). Near the estuary mouth, PIV particles occasionally clumped together, which resulted in incorrect flow measurements that were excluded from comparison with the model. On the other hand, PIV measurements at shallow locations were discontinuous since the PIV particles either stranded on the bars or were drained to deeper waters. Consequently, flow velocity measurements on and around bars tend to be inaccurate, which explains the larger contrast of modelled and measured velocities for shallower areas (Figs.~\ref{fig:FlowComp},~\ref{fig:FlowDepthDiagram}). For example, the model clearly shows the wetting and drying of a tidal bar with peak flow velocities half of those in a bordering channel (Fig.~\ref{fig:FlowDepthDiagram}b). The measurements in the channel are about similar, but are unrealistic for the tidal bar; the PIV measurements suggest negligible flow which is incongruent with the recorded tidal water depth variations.

Residual flow maps of both modelled and measured flow show the expected ebb-dominance of channels and flood-dominance of bars, especially at their seaward sides (Fig.~\ref{fig:ResidualFlow}). Also, the two circulation cells measured on the ebb-tidal delta are well-reproduced by the model. However, the overall modelled residual flow is slightly less flood-dominated (MBE is positive) than the PIV-based residual flow. For example, the flood-dominance of the channel at $x=14$~\unit{m} is weaker but still recognisable in the modelled data (Fig.~\ref{fig:ResidualFlow}). Further landward, a discrepancy arises in that the model suggests that the channel and bar between $x=4$~\unit{m} and 6~\unit{m} are flood-dominant, while the measurements show they are mainly ebb-dominant. Inspection of the raw PIV data shows that here the flood flow is underseeded with particles, suggesting that the measured data is inaccurate and leaving the model untested in this zone.

% - A higher roughness results in smaller flow velocities and smaller differences between high and low tide water levels.

\begin{figure}[b!]
\centering
\includegraphics[width=12.5cm]{TidalPrism.png}
\caption{Tidal prism along the estuary based on experimental data, bathymetry and the model scenarios. Measured flow velocities were converted to depth-averaged velocities using Eq.~(\ref{eq:depthprofile}). Tidal prism based on bathymetry (black dashed line) was computed as the cumulative volume of water along the estuary between high and low water levels imposed at the weir (i.e. with an amplitude of 4~\unit{mm}) \cite[cf.][]{Braat2018}; this calculation ignores effects of friction and river inflow.}
\label{fig:tidalprism}
\end{figure}

%%%
%%%%%%%%%% DISCUSSION %%%%%%%%%%%%%%%%%%%%%%%%%%%%%%
%%%
\section{Discussion}
\subsection{}
The numerical hydrodynamic model Nays2D reproduces water depths and flow velocities for physical scale experiments with both unidirectional and reversing shallow flow (Figs.~\ref{fig:WaterDepthComp},~\ref{fig:FlowComp},~\ref{fig:ResidualFlow}).
~~Modelled water depths are within a~~The mean absolute error of modelled water depth is within 10~\% maximum water depth (Fig.~\ref{fig:ScatterClasses}) and of modelled flow ~~velocities~~velocity is within ~~a mean absolute error of~~ 15~\% maximum flow velocity (Fig.~\ref{fig:SurfaceFlow}). In other

words, the errors of modelled flow fall within the range of errors that ~~is~~ was expected in the measured data. The model results are valuable because the spatio-temporal coverage and quality of experimental data are at present more limited in typical laboratory conditions for landscape experiments. Therefore, this experimental data-model integration opens up many opportunities for the analyses of hydrodynamics in experiments in a time-efficient, cost-effective and labour-inexpensive manner. Thus far, this integration has only been used to the authors' knowledge for one set of tidal scale experiments with erodible boundaries by \cite{Tesser2007} and \cite{Stefanon2010,Stefanon2012}, who numerically computed flow velocity fields by solving the Poisson boundary value problem \citep{Marani2003}. In addition to their findings, the results of this study demonstrate that an experimental data-model integration extends to complex bathymetries with unsteady, nonuniform flows.

~~A major advantage of numerically modelled flow fields is the full coverage and the independence from imperfect lighting, particle seeding and empirical relations through which flow properties are inferred \citep[e.g.][]{VanDijk2013silt,Braat2018}. Additionally, the model adheres to continuity of flow, which is not the case for experimental data with errors, bias and uncertainty.~~ ~~Consequently, the modelled flow fields permit the study of flow partitioning between multiple channels and bars \citep[e.g.][]{BollaPittaluga2003,Kleinhans2008}, as well as of the sensitivity to roughness and turbulence. Additionally, the tidal prism and tidal excursion length can be determined for tidal experiments, which are important system-scale characteristics that are potentially strongly biased~~ ~~by measurement error and missing values in shallow areas (Fig.~\ref{fig:tidalprism}).~~ ~~Higher time resolution and tests of effects of changing boundary conditions can also be quickly accomplished with the model. However, this does not mean that data need no longer be collected because the model requires calibration for e.g. hydraulic roughness.~~

~~The hydraulic roughness is commonly used to calibrate water levels and flow velocities in hydrodynamic models \citep[e.g.][]{Berends2019}. Although a spatially constant Manning roughness of 0.02~\unit{s~m^{1/6}} already produced satisfying hydrodynamics, the results could be improved by calibrating a spatially varying roughness; this is especially the case for experiments with wide sediment distributions or fines \citep[e.g.][]{VanDijk2013silt,Braat2018}.~~ ~~In particular, this~~ ~~may improve the partitioning of water at bifurcations over the downstream channels (for example the secondary channel in the braided river around $x=6$~\unit{m} [Fig.~\ref{fig:WaterDepthComp}]).~~ ~~However, the partitioning of water over channels and bars also depends on which of the three classic assumptions of friction is applied, namely a constant Manning, Chezy or White-Colebrook roughness coefficient (Fig.~\ref{fig:hydraulicRoughness}). For example, using a constant Chezy instead of Manning would result in slightly slower flow in channels and faster flow over bars. In contrast, a constant White-Colebrook would produce faster flow in channels and slower flow over bars. In turn, these differences in flow velocity would have a considerable effect on the computed sediment mobility.~~

\begin{figure}[t!]
\centering
\includegraphics[width=12.5cm]{HydraulicRoughness2.png}
\caption{Effect of different hydraulic roughness predictors on the distribution of depth-averaged flow velocity $\bar{u}$ for (a) a constant Manning, (b) a constant Chezy C and (c) a constant grain roughness k_s (White-Colebrook). The cross-section is from the experimental estuary by \citet{Leuven2018} at $x=15.3$~\unit{m} at maximum tilt in the ebb direction. Cross-sectional flow velocities were iterated for C and k_s assuming the same total discharge and water levels as modelled in this study with Manning.}
\label{fig:hydraulicRoughness}
\end{figure}

\begin{figure}[t!]
\centering
\includegraphics[width=12.5cm]{Figxx_application5.png}
\caption{Complementary model data as maps of nondimensional bed shear stress (i.e. Shields numbers) and tidal zonation. (a)~Shields numbers for the meandering and (b)~braided rivers with (c-d) the corresponding elevation-difference DEMs with the next time step. (e)~Maximum Shields numbers for the estuary in the ebb and (f)~flood direction. (g)~Classification of the estuary DEM in inundation classes based on modelled tidal flow. A similar classification is also applicable to unidirectional flow in rivers, as illustrated in Fig.~S2a,f.}
\label{fig:application}
\end{figure}

A major advantage of numerically modelled flow fields is the full coverage and the independence from imperfect lighting, particle seeding and empirical relations through which flow properties are inferred \citep[e.g.][]{VanDijk2013silt,Braat2018}. Additionally, the model adheres to continuity of flow, which is not the case for experimental data with errors, bias and uncertainty. Consequently, the modelled flow permits a much more accurate calculation of important flow parameters for system scaling and analysis.

One such an example is the computation of tidal prism. Tidal prism based on flow velocity and depth measurements is strongly underestimated by measurement error and missing values in shallow areas (Fig.~\ref{fig:tidalprism}). Alternatively, tidal prism could be computed using bathymetry and the cumulative volume of water between high and low water levels along the estuary, but this method ignores roughness effects and will result in an overestimation of tidal prism if the tide is a propagating wave, as opposed to a standing wave. The drawbacks of these computations are overcome by the model, which shows a steeper decrease of tidal prism in the landward direction due to roughness and a levelling-off towards the landward boundary, indicative of river inflow dominance (Fig.~\ref{fig:tidalprism}). Other important system-scale characteristics that can be derived from the modelled flow are e.g. tidal excursion length \citep[e.g.][]{Schramkowskietal2002} and the flow partitioning between multiple channels and bars \citep[e.g.][]{BollaPittaluga2003,Kleinhans2008}. However, this does not mean that data need no longer be collected because the model may require calibration of e.g. hydraulic roughness.

The hydraulic roughness is commonly used to calibrate water levels and flow velocities in hydrodynamic models \citep[e.g.][]{Berends2019}. Although a spatially constant Manning roughness of 0.02~\unit{s~m^{1/6}} already produced satisfying hydrodynamics, the results could be improved by calibrating a spatially varying roughness; this is especially the case for experiments with wide sediment distributions or fines \citep[e.g.][]{VanDijk2013silt,Braat2018}. Such roughness maps could be generated from grain size maps based on overhead imagery, provided measurement errors due to lighting and sediment colour are greatly reduced. Using a spatially varying roughness may improve the partitioning of water at bifurcations over the downstream channels (for example the secondary channel in the braided river around $x=6$~\unit{m} [Fig.~\ref{fig:WaterDepthComp}]). However, the partitioning of water over channels and bars also depends on which of the three classic assumptions of friction is applied, namely a constant Manning, Chezy or White-Colebrook roughness coefficient (Fig.~\ref{fig:hydraulicRoughness}). For example, using a constant Chezy instead of Manning would result in slightly slower flow in channels and faster flow over bars. In contrast, a constant White-Colebrook would produce faster flow in channels and slower flow over bars. In turn, these differences in flow velocity would have a considerable effect on the computed sediment mobility.

Sediment mobility is perhaps the most important measure of flow for morphodynamics \citep{KleinhansBerg2011} (Fig.~\ref{fig:application}), but it is difficult to acquire from experiments with shallow flow. Firstly, the nondimensional mobility number allows for the comparison to natural systems \citep{Kleinhans2010}. Secondly, it provides vital insight in sediment transport fields and morphological activity that is especially valuable for studying multi-channel systems and channel-bar margin interactions \citep{deVet2017,VanDijk2018,Baar2019Nature}. For example, these data may be used to predict future locations of erosion and deposition (Fig.~\ref{fig:application}a-d). Also, they may be indicative of grain size or may be coupled to grain size estimations from imagery \citep[e.g.][]{Gardner2011}.

The model is potentially applicable in conditions where data collection is hampered, such as in vegetated experiments \citep[e.g.][]{Braudrick2009,TalPaola2007,TalPaola2010}. Application on vegetation surfaces ~~may require that~~requires the vegetation ~~is~~to be filtered out of the DEMs and ~~that~~ vegetation roughness effects ~~are~~to be added to the model \citep{Baptist2007,Weisscher2019Meander}. Consequently, experimental data ~~may~~could be enriched with water depth maps and particularly flow fields that are often absent (Table~\ref{tab:exp_measurements}).

Water depth and sediment mobility maps enable unbiased classification of a river or estuary planform into inundation zones (Fig.~\ref{fig:application}g). For instance, this enables the study of the development of intertidal areas in estuaries, which are of key importance to a high biodiversity \citep[e.g.][]{Ysebaert2003}. Moreover, such inundation classifications may effectively culminate in ecotopic maps that indicate at what locations which faunal and floral species would be likely to thrive.

Finally, the model opens up a faster way of testing the design of a flume experiment. Whilst laboratory tests need to be done in series, the model allows for testing initial and boundary conditions in parallel. Based on the resulting flow fields and bed shear stress maps at the start of the modelled flume setups (sediment transport is not included), preferred flume settings may be readily derived and applied to the physical flume. Therefore, probably fewer physical tests are required, which greatly reduces the total laboratory time. This is especially the case for experiments with different sediment mixtures and with vegetation, for which the flume needs to be emptied and cleaned after every run.

%%
%%%%%%%%%% CONCLUSION %%%%%%%%%%%%%%%%%%%%%%%%%%%%%
%%
\section{Conclusion}
Hydrodynamic modelling with Nays2D simulates unsteady, nonuniform flows for physical scale experiments with unidirectional and reversing shallow flow. The modelling requires a DEM and the corresponding boundary conditions and produces continuous spatio-temporal data on water depth and flow velocity, whilst ignoring substrate colour differences, lighting overexposure and under or oversampling of floating PIV modules that usually decrease the quality of experimental data. Additionally, Nays2D computes sediment mobility, which is normally difficult to measure in shallow flows but is an important parameter for morphological activity and the comparison to natural systems.

The implication of this experimental data-model integration is that fewer measurements and less post-processing are required and are mainly meant for the calibration of model parameters such as

the hydraulic roughness. In turn, this integration opens up many opportunities for the analyses of hydro and morphodynamics in experiments. For example, the enhanced data enable the objective classification of the experiment planform into inundation classes which are potentially indicative of different ecotopes. Alternatively, the model allows for rigorous testing of different boundary conditions (e.g. discharge variability, sea level rise, vegetation) which could strongly reduce the time in the laboratory.

%%
\dataavailability{Data will be made available upon acceptance of the manuscript and a user manual is provided that explains how Nays2D can be used to augment data of scale experiments. Modelled data in this study were derived from numerical modelling that can be repeated with the open-source Nays2D model available at \url{i-ric.org}. The supplementary materials include the DEMs used in this study, the raw water depth and flow velocity data, the novel Nays2DMetronome solver specifically for tilting flumes, and a user manual for iRIC (i.e., the User Interface for Nays2D).}

\authorcontribution{The authors contributed in the following proportions to concept and design, experimental data collection, modelling, analysis and conclusions, and manuscript preparation:
SAHW(50, 0, 80, 60, 70~\%),
MBA(20, 0, 20, 10, 5~\%),
JRFWL(10, 40, 0, 10, 10 \%),
WMvD(0, 40, 0, 10, 5~\%),
YS(10, 0, 0, 0, 0~\%),
MGK(10, 20, 0, 10, 10~\%).}

\competinginterests{The authors declare that they have no conflict of interest.}

% \disclaimer{TEXT} %% optional section

\begin{acknowledgements}
~~We will acknowledge reviewers. Weisscher, Boechat-Albernaz and Kleinhans were~~This research is supported by the European Research Council through the ERC Consolidator grant 647570 to M.G. Kleinhans~~. Leuven~~ and ~~Van Dijk were supported by~~ the Dutch Technology Foundation STW ~~(~~grant Vici 016.140.316/13710 to M.G. Kleinhans, which is part of the Netherlands Organisation for Scientific Research~~, grant Vici 016.140.316/13710) to Kleinhans~~. This work is part of the Ph.D. research of S.A.H. Weisscher. We acknowledge L. Lacaze and M. Tal, whose reviews helped to improve the manuscript.
\end{acknowledgements}

%%
%%%%%%%%%% REFERENCES %%%%%%%%%%%%%%%%%%%%%%%%%%%%%
%%
\bibliographystyle{copernicus}
\bibliography{Database_SAH_Weisscher.bib}

\end{document}